

Astronomical imaging using ground-layer adaptive optics

Christoph Baranec, Michael Lloyd-Hart, N. Mark Milton, Thomas Stalcup,
Miguel Snyder, Vidhya Vaitheeswaran, Don McCarthy, and Roger Angel
Center for Astronomical Adaptive Optics, Steward Observatory,
933 N. Cherry Ave., Tucson, AZ, 85721

ABSTRACT

Over the past several years, experiments in adaptive optics involving multiple natural and Rayleigh laser guide stars have been carried out by our group at the 1.5 m Kuiper telescope and the 6.5 m MMT telescope. From open-loop data we have calculated the performance gains anticipated from ground-layer adaptive optics (GLAO) and laser tomography adaptive optics corrections. In July 2007, the GLAO control loop was closed around the focus signal from all five laser guide stars at the MMT, leading to a reduction in the measured focus mode on the laser wavefront sensor by 60%. For the first time, we expect to close the full high order GLAO control loop around the five laser beacons and a tilt star at the MMT in October 2007, where we predict image quality of < 0.2 arc seconds FWHM in K band ($\lambda = 2.2 \mu\text{m}$) over a 2 arc minute field. We intend to explore the image quality, stability and sensitivity of GLAO correction as a function of waveband with the science instrument PISCES. PISCES is a 1-2.5 μm imager with a field of view of 110 arc seconds, at a scale of 0.11 arc seconds per pixel. This is well matched to the expected FWHM performance of the GLAO corrected field and will be able to examine PSF non-uniformity and temporal stability across a wide field.

Keywords: adaptive optics, ground-layer adaptive optics, wavefront sensors, laser guide stars, infrared instrumentation

1. INTRODUCTION

Ground-layer adaptive optics (GLAO) is a potentially powerful adaptive optics (AO) technique which promises modest wavefront correction over wide fields of view. By measuring and averaging the incoming wavefronts to a telescope at several different field points, an estimate of the common turbulence located near the entrance pupil of the telescope can be made, with the uncorrelated higher altitude contributions averaged away. This estimate, when applied to a deformable mirror conjugated near the telescope's pupil, can correct the atmospheric aberration close to the telescope which is common to all field points. It has been found empirically at various sites that typically half to two-thirds of the atmospheric turbulence lies in this ground layer¹⁻⁹, so when the technique is applied, the natural seeing will improve substantially over a large field. This will be of particular value to science programs that until now have not found any advantage in AO. Many observations that are normally carried out in the seeing limit will benefit from improved resolution and signal-to-noise, ultimately increasing scientific throughput.

Ground-layer correction was first suggested by Rigaut¹⁰ as a way to improve wide field imaging for large telescopes. Since then, numerous simulations have shown that GLAO can effectively and consistently improve the atmospheric seeing^{1, 10-13}. GLAO was first demonstrated using three bright natural guide stars on a 1.5 arc minute diameter with the Multi-conjugate Adaptive Optics Demonstrator fielded at the VLT in early 2007. Unfortunately, due to the limited number of suitably bright natural guide star constellations on the sky, the system will not be able to support routine science observations. However, plans are currently underway to implement GLAO at several telescopes around the world with a variety of techniques¹⁴⁻¹⁹.

The MMT multiple laser AO system, after being in development for several years, is currently being commissioned. Its main goals are as a proof of concept for ground-layer adaptive optics and laser assisted tomographic adaptive optics (LTAO) using laser guide stars and to support science observations, providing diffraction-limited imaging in the thermal infrared bands and substantial image improvement in K ($\lambda = 2.2 \mu\text{m}$) and shorter bands over all the sky accessible above 45° elevation. In addition, actual on-sky GLAO and LTAO correction performance will be evaluated. In previous open-loop experiments, all performance estimates were based on wavefront measurements from the different wavefront sensor cameras. With a closed-loop system sending AO corrected light to science cameras, the imaging improvement can be directly measured and the parameters which affect correction can be explored. This will

lead to a greater understanding of the important factors in upgrading the MMT's laser AO system and for supporting the design of adaptive optics systems for the 2×8.4 m Large Binocular Telescope¹⁹ and the 25 m Giant Magellan Telescope²⁰⁻²².

2. MMT MULTIPLE LASER AO SYSTEM

The MMT's multiple laser guide star (LGS) AO system is comprised of four main components: the laser beam projector, a Cassegrain mounted wavefront sensor, a real-time reconstructor computer and the adaptive secondary mirror^{23, 24}.

The laser beam projector has been in use since June 2004 and has supported several open-loop observing runs²⁵. The system projects five Rayleigh LGS from behind the secondary of the MMT into a regular pentagon of beacons on the sky with a radius of 60 arc seconds. These beacons are dynamically focused in the return optics²⁶ from an elevation of 20 to 29 km above the telescope, increasing the telescope's depth of field, increasing the photon return. It has been found that wind driven oscillations in the secondary hub, where the beam projector is housed, can cause excessive jitter of the laser beams, corrupting the wavefront sensor measurements. This has been recently addressed with accelerometers placed on the secondary hub commanding a fast steering mirror in the beam projector optics²⁵.

For a more thorough description of the wavefront sensing instrument pictured in figure 1, see Baranec²⁷. Although the basic design is similar to that used in previously published experiments^{4, 5}, the wavefront sensing instrument was reengineered in early 2006²⁸ in anticipation of closed-loop work during 2007. The images from all five laser beacons are recorded on a novel implementation of the Shack-Hartmann wavefront sensor (WFS), which includes the dynamic focus optics and a single electronically shuttered CCD. A prism array divides the pupil into 60 subapertures of equal area arranged in a hexapolar geometry. Substantial improvements to the optics have been made, increasing throughput and SNR, allowing the LGS WFS to run at a faster 460+ frames per second. In addition, three other cameras are installed in the instrument: a fast tip-tilt camera with a searchable 2 arc minute field using an electron multiplying L3 CCD, a standard 12×12 natural guide star Shack-Hartmann wavefront sensor which can be used for open-loop testing or other calibrations, and a wide field video camera used for acquisition. The instrument was also designed as a modular drop in replacement for the MMT's NGS AO wavefront sensing instrument and preserves many of the same features including support for the suite of current F/15 science instruments at the MMT: PISCES²⁹, Clio^{30, 31}, ARIES³² and BLINC-MIRAC³³.

The real-time reconstructor computer reads frames from the laser wavefront sensor and tilt sensor and computes corrections to be applied to the adaptive secondary mirror. Beginning in 2007, a new PC based reconstructor computer, developed in-house, was fielded for use with the laser AO system. Originally designed to support the NGS AO system, it has now been modified to accommodate the LGS WFS in ground-layer AO mode, where the slopes from corresponding subapertures are averaged before being multiplied by the reconstructor matrix. It consists of dual quad core Xeon X5355 CPUs running at 2.66 GHz, with 2GB of memory. The PC reconstructor is programmed in C under the CentOS operating system with RTAI real-time extensions, and uses an EDT PCI-DV framer grabber card for communication with the laser wavefront sensor controller. The PC reconstructor is currently being used as the baseline reconstructor for GLAO mode; however, to support LTAO, where a much larger reconstruction matrix multiply needs to be performed, the PC reconstructor will need to be expanded to a parallel processing architecture.

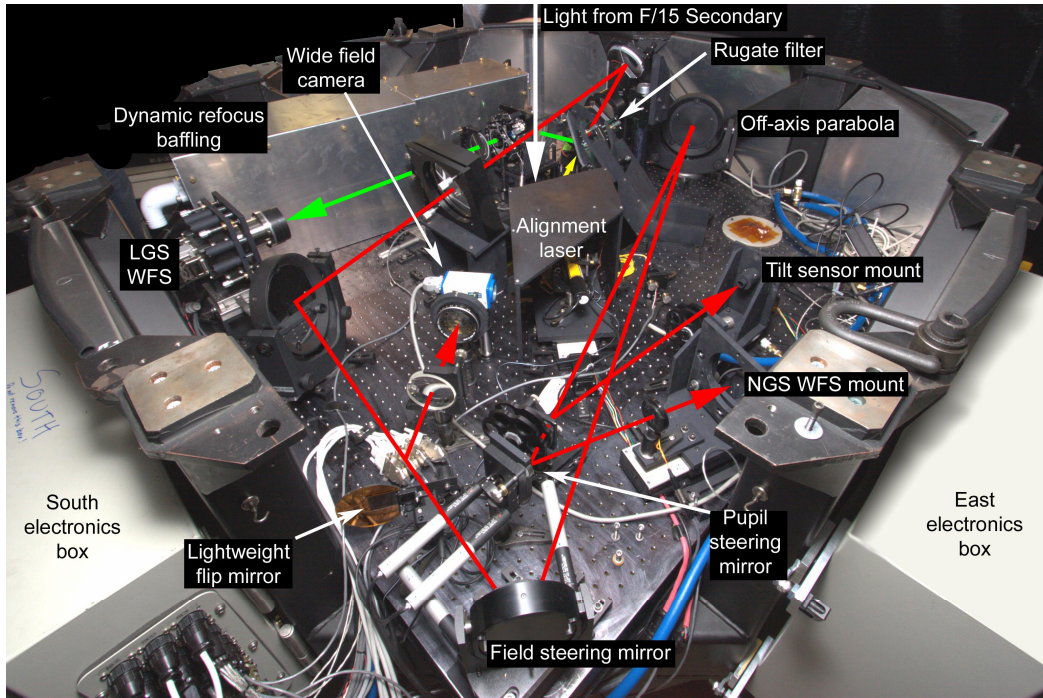


Fig. 1. Photograph of the wavefront sensing instrument as built in July 2007. The main white arrow shows the light coming off of the F/15 adaptive secondary. The yellow arrow shows the visible light reflected off of the tilted dichroic / science instrument entrance window. The green arrow shows the path of the $\lambda = 532$ nm reflected off of the rugate filter into the laser wavefront sensor. The red arrow shows the remaining visible light as it passes to the tilt, wavefront sensor and wide field cameras.

3. OPEN-LOOP GROUND-LAYER AO RESULTS

For a full description of the results of open-loop wavefront sensing with multiple guide stars, we refer the reader to previously published accounts^{4, 5, 34, 35}. Open-loop wavefront sensing of four natural guide stars at the 1.5 m Kuiper telescope have found that the wavefront aberration in each star can be roughly halved by subtracting the average of the wavefronts from the other three stars. Wavefront correction on this basis leads to a reduction in width of the seeing-limited stellar image by up to a factor of 3, with image sharpening effective from the visible to near-infrared wavelengths over a field of at least 2 arc minutes.

At the MMT, open-loop measurements of ground-layer AO have been performed over several observing runs since September 2004. An estimate of the ground-layer turbulence is calculated as the average of the five reconstructed laser wavefronts. The Zernike amplitude coefficients are calculated, averaged and compared to the coefficients of a stellar wavefront and the residual is used to predict ground-layer AO correction. Table 1 shows example data sets of open-loop ground-layer AO correction, excluding tilt. For each ~ 1 minute data set, the raw stellar wavefront error measured is compared to the estimated wavefront error after ground-layer correction. Atmospheric parameters, r_0 and L_0 , during the times of each observation are also presented.

Table 1. Example RMS wavefront error before and after open-loop ground-layer AO correction with the laser guide stars.

	Sept. '04	June '05 (1)	June '05 (2)	April '06
Stellar RMS wavefront error	645 nm	374 nm	511 nm	448 nm
RMS wavefront error after GLAO correction	397 nm	290 nm	360 nm	249 nm
% RMS correction	38 %	23 %	30 %	44 %
Zernike orders used	2-6	2-6	2-8	2-8
r_0 (at $\lambda = 500$ nm)	12.6 cm	22.6 cm	14.8 cm	18.0 cm
L_0	19.6 m	14.4 m	12.0 m	12.5 m
Frame rate (fps)	50	100	100	200

PSF simulations were done for the data exploring the ground-layer AO field from June 2005 (1) from the measured and residual stellar wavefront information. These simulations included a temporal lag of 0.02 seconds (2 frames). Synthetic residual tilt errors were also added assuming that global image motion was measured from a natural star at the center of the field, with noise and anisoplanatic errors determined empirically from separate observations of a five star asterism on the tilt camera. The seeing limited PSF FWHM, 0.36 and 0.34 arc seconds at H ($\lambda = 1.65 \mu\text{m}$) and K bands respectively, drops to a range of 0.10 to 0.14 arc seconds after GLAO correction depending on distance from the center of the laser beacon constellation.

Even though the seeing was already excellent for the June 2005 (1) data, ground-layer AO further improved the resolution, to within about a factor 2 of the diffraction limit. θ_{50} , the radius within which 50% of the total PSF energy is contained, also saw substantial improvement, particularly in the K band. Furthermore, the variability of the PSF over the explored field, with a radius of 50 arc seconds, is remarkably small. While these results by themselves are encouraging, the value of ground-layer AO is not restricted to periods when the seeing is already good. Unlike conventional AO where the diffraction limit is the goal, the more modest reach of ground-layer AO is also more robust to adverse atmospheric conditions. Data from September 2004 when the value of r_0 was 10.1 cm, approximately half the value for the results in June 2005 (1), show that improvement of the K-band PSF to FWHM of 0.2 arc seconds will still be possible under such conditions.

4. OPERATION OF THE CLOSED-LOOP SYSTEM

As a new system at the MMT, the operation and implementation of the closed-loop laser AO system is a continually evolving process. The first step is the alignment of the telescope and science camera. The adaptive secondary mirror is set to the 'flat' position. This position most closely resembles a non-aberrated aspheric shape and is based on off-telescope calibrations. The telescope is then collimated, using feedback from the science camera.

The next step is to calibrate the laser wavefront sensor camera. First, a bright star is placed on the natural guide star wavefront sensor and the loop is closed with this system. This reduces most of the effect of the atmosphere and provides a less aberrated path between the laser beacons and the laser wavefront sensor. While the NGS loop is closed, images of the laser beacons are recorded on the laser wavefront sensor over a period of a minute or more. The images are averaged and the centroid position of each Shack-Hartmann spot is calculated. These will be used as the zero mean position of the spots. This can be done without the natural guide star sensor, using just the flat position of the mirror, but more of the non-common path errors will be taken out if the closed-loop NGS system is used in the calibration. With the mean spot positions calculated on the laser wavefront sensor, a 4×4 pixel sub-image for each spot is identified. The slopes are then calculated from the averaged laser wavefront sensor frame and are saved as slope offsets and sent to the PC reconstructor along with the subaperture locations. A background frame is also taken with the laser beacons turned off and sent to the PC reconstructor.

The PC reconstructor is then ready for closed-loop operation. Frames from the laser wavefront sensor are sent directly to the reconstructor. Each frame is processed by first applying a background subtraction. Slopes are then calculated for each subaperture and the offset is removed. The vector of slopes is then pre-multiplied by a reconstructor matrix and commands to the adaptive secondary mirror are produced. A multiplicative factor, called the system gain, is applied to the commands sent to the adaptive mirror. When the loop is first closed, this is set to zero. It is slowly increased until the loop appears stable. Typically, gains of 0.5 are used, but this is the focus of ongoing research.

The full procedure detailed has yet to be implemented. In July 2007 the laser AO loop was closed; however, with very limited sky time, the calibration of the laser wavefront sensor with the closed-loop natural guide star system was skipped. This will be required in future observing runs when the system performance will be analyzed in more detail.

5. CLOSED-LOOP LAB TESTS

Original testing and calibration of the adaptive F/15 secondary mirror was done using the ‘Shimulator’ test setup³⁶. In 2003, the Shimulator was decommissioned and the development of a new compact replacement test setup, based on the Hindle test, had begun. It was completed in the summer of 2007, as seen in figure 2, and although it was originally built to update the calibrations of the secondary mirror, it could also be used to test closed-loop operation of the laser wavefront sensor in conjunction with the PC based reconstructor computer. The new test setup includes the use of a 4-D interferometer to measure the surface of the adaptive secondary mirror, and was modified to use a pellicle beam splitting mirror to pick off part of the returning light to the interferometer. This light, which is reflected in double-pass off of the adaptive secondary mirror, is then relayed to the laser wavefront sensor. The PC reconstructor was set to receive signals from the wavefront sensor, calculate mirror commands and send them to the secondary mirror. In this way, an optical feedback loop between the mirror and the wavefront sensor is established.

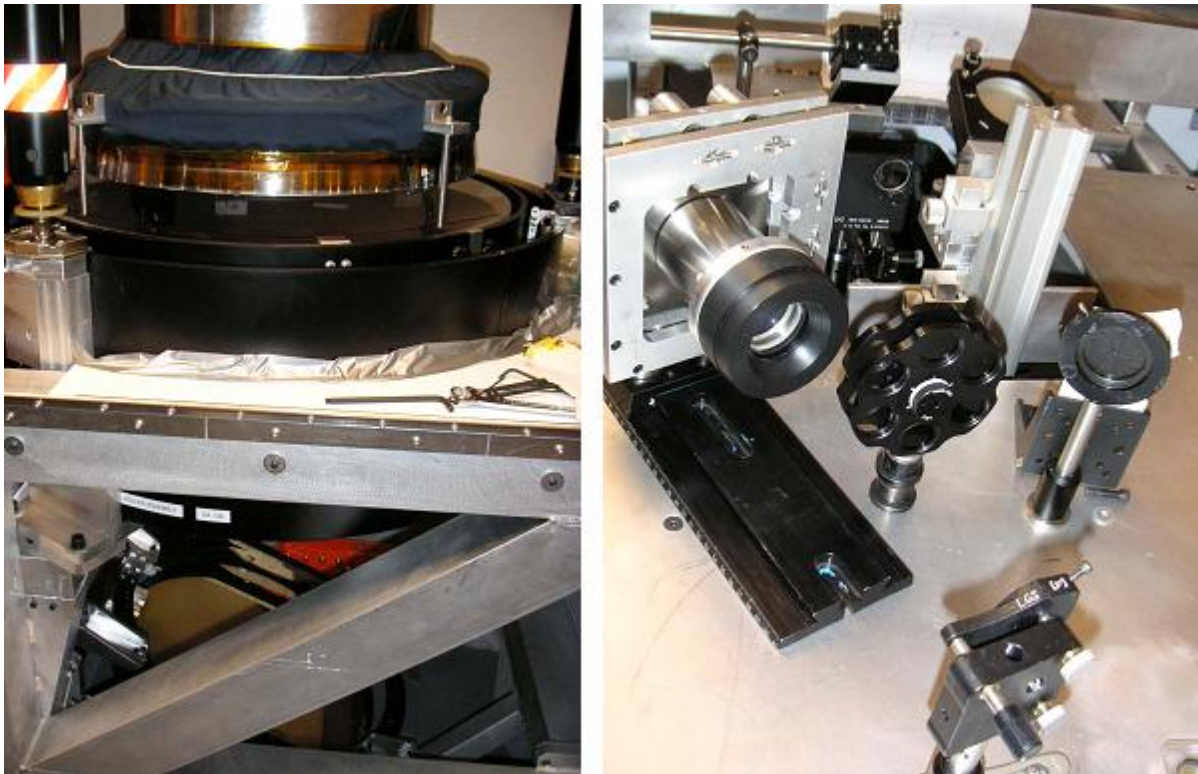


Fig. 2. Test stand environment with the F/15 adaptive secondary mirror (left) integrated with the laser guide star wavefront sensor (right).

In this setup, since there was only a single source produced by the interferometer, the reconstructor was adapted to use only information from the one illuminated beacon. The extension to multiple beacons is in principle trivial. Initially, the focus only loop was closed at 30 Hz and it was found that the sign of the correction was wrong. Once set properly, the focus loop remained stable. Next, astigmatism and trefoil were added to the control space until the rotation of the reconstructor matrix was determined properly. Once this had been determined, the full Zernike order 1 through 8 reconstructor was used and the loop remained closed for over 10 minutes. The loop was then closed for five minutes at 200 Hz before the tests were determined to be a complete success. The test stand work had demonstrated that issues with the software had been resolved and any remaining obstacles to closing the loop on-sky would have to be discovered during observations.

6. JULY 2007 OBSERVATIONS

The latest attempt at closing the adaptive optics loop occurred in July of 2007 for 4 nights. The run was almost entirely lost due to weather, but about four hours were usable. During that time, the tip/tilt loop using a natural guide star was again closed to confirm the system was still working. Subsequently, the laser loop was closed around a focus only reconstructor for the first time. Shortly after this success, the clouds rolled in and there were no more clear skies for the rest of the run.

On July 8th 2007, the adaptive optics control loop was closed around the ground-layer focus signal from the laser guide stars. Telemetry data was recorded on the PC reconstructor; although it appears that every other data frame from the laser guide star wavefront sensor were not recorded. The seeing conditions at the time of observations, calculated from the uncorrected laser modes and independent PISCES images, were: $r_0 = 8.1$ cm, the 88th percentile of seeing, and $L_0 = 19$ m.

After calibration of the laser wavefront sensor camera using the flat position of the adaptive secondary mirror, the hexapod holding the mirror was moved $20 \mu\text{m}$ towards the primary mirror. This added a static offset of -426 nm of Zernike focus for the AO system to correct in addition to atmosphere. Figures 3 and 4 show the measured ground-layer focus and 45° astigmatism modes as recovered from the recorded slope information from a single data set on the laser wavefront sensor. The data show every other frame while the system was running at ~ 208 Hz. The control loop gain, a user defined multiplicative factor applied to the adaptive mirror commands, was initially set to zero, set to 0.2 at 12.5 s and incrementally increased to 0.9. As can be seen in figure 3, the measured focus mode moves towards a mean value of 0 nm when the loop gain is increased from zero, correcting the static offset added with the movement of the hexapod.

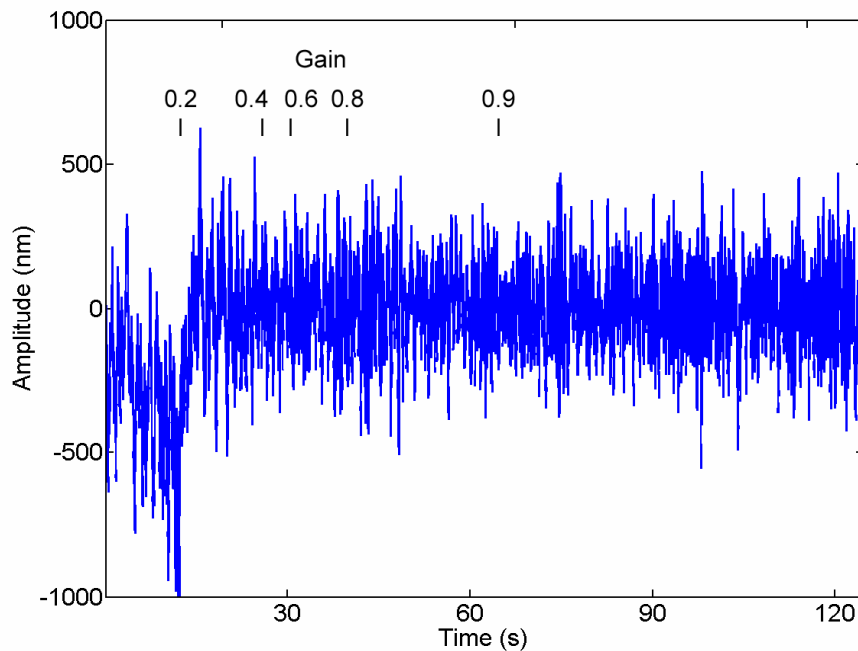


Fig. 3. Measured ground-layer focus mode during closed-loop correction of focus. The tick marks show when the gain factor, which starts at zero at time = 0 s, increases to a new value.

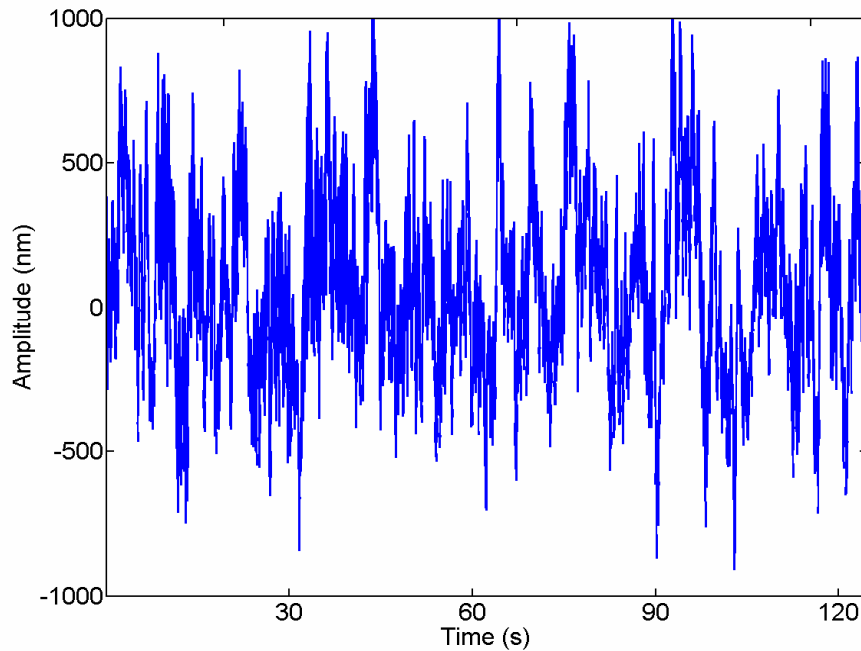


Fig. 4. Measured simultaneous ground-layer astigmatism mode during closed-loop correction of focus.

The RMS wavefront error in astigmatism during the closed loop correction focus was 341 nm. Since both astigmatism and focus modes are from the same Zernike radial order, they should have the same statistics. Over the first 12.5 seconds, when the gain was still set to zero, and assuming a mean value set by the offset of -426nm, the RMS focus error is 265 nm; the difference due likely to small number statistics of temporally correlated data. Table 2 lists the RMS wavefront error measured as a function of gain value. After the control loop was closed and the gain set to 0.9, the wavefront error in focus drops to 130 nm RMS, approximately a 60% reduction compared to the uncompensated astigmatism mode. This is comparable to the estimated wavefront improvement of ground-layer AO correction of a natural star^{4, 5, 34}.

Table 2. RMS wavefront error during closed-loop correction of focus as a function of gain factor. *Focus of zero gain assumed a mean value of -426 nm.

Mode	Gain	RMS (nm)	Number of frames
Astigmatism	0	341	12965
Focus	0	265*	1301
	0.2	190	1352
	0.4	127	520
	0.6	142	936
	0.8	144	2600
	0.9	130	6256

Figure 5 shows the power spectra of the modes shown in figures 3 and 4 during closed-loop operation. The focus power spectrum is split into times of low gain (0.2, 0.4 and 0.6) and high gain (0.8 and 0.9). The ground-layer AO loop is correcting for power in focus below ~ 2 Hz, with greater correction occurring with a higher gain factor. There is a spike in the spectra at 13.7 Hz due to vibrations in the secondary hub.

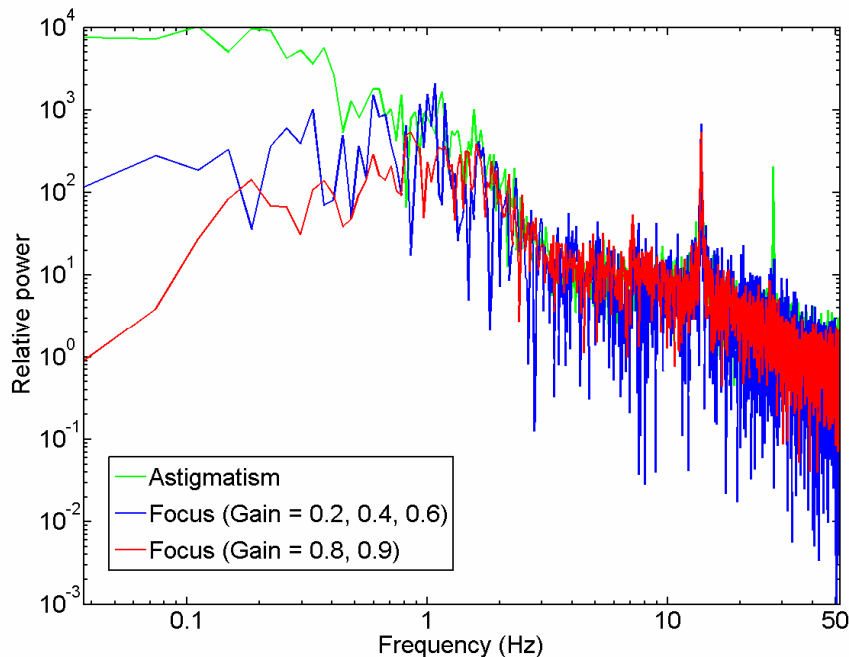


Fig. 5. Power spectrum of astigmatism (green), focus at low gain (0.2, 0.4 and 0.6; blue) and focus at high gain (0.8 and 0.9; red) during closed-loop correction of focus.

The commanded focus position of the adaptive secondary mirror has also been recorded. This appears in figure 6 along with the times the gain factor was changed. The mean position of the mirror during non-zero gain is -202 nm. Because of the factor of two between the mirror shape and the optical path difference added by the mirror, it is compensating for -404 nm of static defocus; agreeing to within 5% of the -426 nm added by moving the hexapod 20 μm prior to increasing the loop gain from zero.

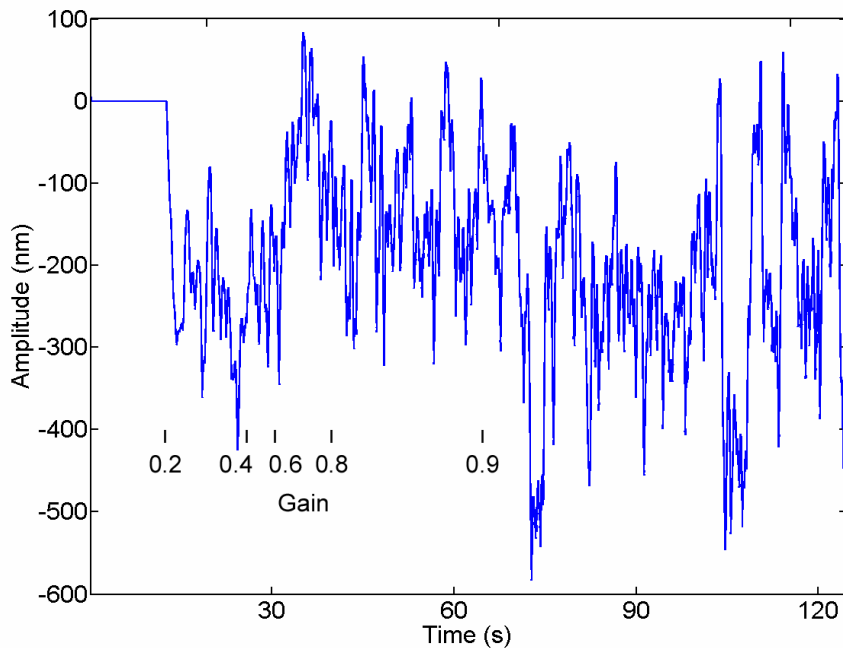


Fig. 6. Adaptive mirror command of focus mode during closed-loop correction of focus.

The power spectrum of the commanded focus position of the adaptive secondary mirror has also been calculated and appears in figure 7. The spectrum has been calculated during times of low and high gain. With a higher gain factor, the adaptive mirror is putting more power into higher frequencies, above ~ 1 Hz, with no noticeable noise floor. It is currently unclear why this increased amount of correction in the higher frequencies does not show up in the power spectrum of the corrected focus mode (figure 5); however it may be addressed in the future with a more intelligent controller than is currently implemented at the MMT^{37,38}.

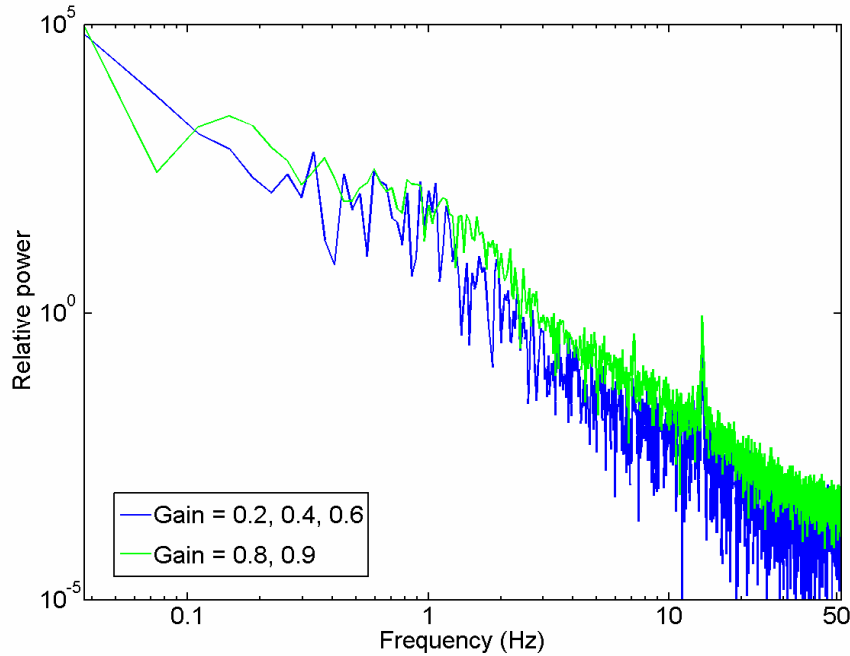


Fig. 7. Power spectra of the adaptive mirror command of focus mode with low gain (blue) and high gain (green) during closed-loop correction of focus.

With the limited time available, ground-layer adaptive optics with laser guide stars has been demonstrated for the first time. With the poor seeing and the control of a single mode, it is impossible to see any imaging improvement on the PISCES science camera. However, the reduction in power of the focus mode during closed-loop operation clearly show that the system and technique have been successfully implemented and full high order correction is only a few steps away.

7. CONCLUSIONS AND FUTURE WORK

The next step is to go back to the MMT and test the closed-loop system again. Four nights have been allotted for the system in October 2007. During this observation run, it is intended to close the full high order laser ground-layer AO loop simultaneously with the tip/tilt loop on a natural guide star. The imaging stability, sensitivity and improvement over a 110 arc second field will be explored with PISCES as its plate scale is well matched to the expected ground-layer performance. In a subsequent observing run, narrow field PSF characterization will be done using Clio, in the thermal infrared of $\lambda = 3.5$ and $4.8 \mu\text{m}$, with Nyquist sampling of 0.048 arc seconds per pixel. Strehl ratios of 30 to 40% are expected at $4.8 \mu\text{m}$ in median seeing conditions.

Imaging with both cameras will allow for the exploration of parameters which affect the ground-layer AO correction. In particular, variables such as control gain, reconstruction basis set and the number of controlled modes need to be optimized. The effect of observing conditions, such as the brightness and field location of the tilt star, also need to be explored so future science programs can anticipate the imaging performance of the ground-layer AO correction.

Looking forward to future tomographic AO correction at the MMT, calibrations will also be made for the optical system. The adaptive secondary mirror will be commanded to static shapes and their influence on the measured wavefront of each laser beacon will be recorded. This will map out the pupil from each beacon as it is seen through the Shack-Hartmann lenslet array and will allow for increased reconstruction fidelity.

Early application to scientific programs will focus on seeing improvement with GLAO, taking advantage of existing near infrared instrumentation²⁸. This choice is motivated by a number of considerations. Not only is GLAO the easiest multi-beacon technique to implement, but the MMT's system is likely to remain unique for several years. The exploitation of routine near infrared seeing of 0.2 arc seconds or better over a field of several arcminutes is likely to be very productive, both for imaging and high resolution multi-object spectroscopy (MOS) where the many-fold improvement in encircled energy within 0.2 arc seconds will be of particular value. In addition, a new high-resolution near-infrared wide field camera, Loki, with both imaging and MOS capabilities, is being designed specifically to take advantage of the wide corrected field afforded by the MMT's ground-layer adaptive optics system³⁹.

Observations reported here were made at the MMT, a joint facility of the University of Arizona and the Smithsonian Institution. We are grateful for assistance from Matt Rademacher and for the continued support of the MMT Observatory staff, particularly Mike Alegria, Allie Milone and John McAfee. This work has been supported by the Air Force Office of Scientific Research under grant F49620-01-1-0383 and the National Science Foundation under grant AST-0138347.

REFERENCES

1. D. Andersen, J. Stoesz, S. Morris, M. Lloyd-Hart, D. Crampton, T. Butterley, B. Ellerbroek, L. Jollissaint, N. M. Milton, R. Myers, K. Szeto, A. Tokovinin, J.-P. Veran & R. Wilson, "Performance Modeling of a Wide-Field Ground-Layer Adaptive Optics System," *Publ. Astron. Soc. Pac.* 118, 1574-1590 (2006).
2. R. Avila, E. Masciadri, J. Vernin & J. Sánchez, "Generalized SCIDAR Measurements at San Pedro Mártir. I. Turbulence Profile Statistics," *Publ. Astron. Soc. Pac.* 116, 682-692 (2004).
3. S. Egner, E. Masciadri, D. McKenna, T. M. Herbst & W. Gaessler, "G-SCIDAR measurements on Mt. Graham - recent results," *Proc. SPIE Advances in Adaptive Optics II*, eds. B. Ellerbroek & D. B. Calia, 6272 (2006).
4. M. Lloyd-Hart, C. Baranec, N. M. Milton, T. Stalcup, M. Snyder, N. Putnam, & J. R. P. Angel, "First tests of wavefront sensing with a constellation of laser guide beacons," *Astrophys. J.* 634, 679-686 (2005).
5. M. Lloyd-Hart, C. Baranec, N. M. Milton, M. Snyder, T. Stalcup & R. Angel, "Experimental results of ground-layer and tomographic wavefront reconstruction from multiple laser guide stars," *Opt. Express* 14, 7541-7551 (2006).
6. A. Tokovinin & T. Travouillon, "Model of optical turbulence profile at Cerro Pachón," *Mon. Not. R. Astron. Soc.*, 365, 1235-1242 (2006).
7. A. Tokovinin, J. Vernin, A. Ziad & M. Chun, "Optical Turbulence Profiles at Mauna Kea measured by MASS and SCIDAR," *Publ. Astron. Soc. Pac.* 117, 395-400 (2005).
8. V. Velur, R. Flicker, B. Platt, M. Britton, R. Dekany, M. Troy, J. Roberts, J. Shelton & J. Hickey, "Multiple guide star tomography demonstration at Palomar Observatory," *Proc. SPIE Advances in Adaptive Optics II*, eds. B. Ellerbroek & D. B. Calia, 6272 (2006).
9. J. Verin, A. Agabi, R. Avila, M. Azouit, R. Conan, F. Martin, E. Masciadri, L. Sanchez, & A. Ziad, "Gemini site testing campaign. Cerro Pachon and Cerro Tololo," Gemini RPT-AO-G0094, <http://www.gemini.edu/> (2000).
10. F. Rigaut, "Ground-conjugate wide field adaptive optics for the ELTs," *Proc. ESO Beyond Conventional Adaptive Optics*, eds. E. Vernet, R. Ragazzoni, S. Esposito & N. Hubin, 58, 11-16 (2002).
11. M. Le Louarn & N. Hubin, "Improving the seeing with wide-field adaptive optics in the near-infrared," *Mon. Not. R. Astron. Soc.* 365, 1324-1332 (2006).
12. A. Tokovinin, "Ground layer sensing and compensation," *Proc. SPIE Second Backaskog Workshop on Extremely Large Telescopes*, eds. A. L. Ardeberg & T. Andersen, 5382, 490-499 (2004).
13. A. Tokovinin, "Seeing improvement with ground-layer adaptive optics," *Publ. Astron. Soc. Pac.* 116, 941-951 (2004).
14. R. Stuik, R. Bacon, R. Conzelmann, B. Delabre, E. Fedrigo, N. Hubin, M. Le Louarn & S. Strobele, "GALACSI - The ground layer adaptive optics system for MUSE," *New Astron. Rev.* 49, 618-624 (2006).
15. M. Casali, J.-F. Pirard, M. Kissler-Patig, A. Moorwood, L. Bedin, P. Biereichel, B. Delabre, R. Dorn, G. Finger, D. Gojak, G. Huster, Y. Jung, F. Koch, J.-L. Lizon, L. Mehrgan, E. Pozna, A. Silber, B. Sokar & J. Stegmeier,

- “HAWK-I: the new wide-field IR imager for the VLT,” Proc. SPIE Ground-based and Airborne Instrumentation for Astronomy, eds. I. McLean & M. Iye, 6269 (2006).
16. A. Tokovinin, S. Thomas, B. Gregory, N. van der Blik, P. Schurter, R. Cantarutti & E. Mondaca, “Design of ground-layer turbulence compensation with a Rayleigh beacon,” Proc. SPIE Advancements in Adaptive Optics, eds. D. Bonaccini Calia, B. Ellerbroek, & R. Ragazzoni, 5490, 870-878 (2004).
 17. K. Szeto, D. Andersen, D. Crampton, S. Morris, M. Lloyd-Hart, R. Myers, J. Jensen, M. Fletcher, W. R. Gardhouse, N. M. Milton, J. Pazder, J. Stoesz, D. Simons & J.-P. Véran, “A proposed implementation of a ground layer adaptive optics system on the Gemini Telescope” Proc. SPIE Ground-based and Airborne Instrumentation for Astronomy, eds. I. McLean, & M. Iye, 6269 (2006).
 18. R. Ragazzoni, T. Herbst, W. Gaessler, D. Andersen, C. Arcidiacono, A. Baruffolo, H. Baumeister, P. Bizenberger, E. Diolaiti, S. Esposito, J. Farinato, H. Rix, R.-R. Rohloff, A. Riccardi, P. Salinari, R. Soci, E. Vernet-Viard & W. Xu, “A visible MCAO channel for NIRVANA at the LBT,” SPIE Proc. Adaptive Optical System Technologies II, eds. D. Bonaccini Calia & P. Wizinowich, 4839, 536-543 (2003).
 19. M. Lloyd-Hart, R. Angel & R. Green, “Multilaser guide star adaptive optics for the large binocular telescope,” these proceedings.
 20. M. Lloyd-Hart, R. Angel, N. M. Milton, M. Rademacher & J. Codona, “Design of the adaptive optics systems for GMT,” Proc. SPIE Advances in Adaptive Optics II, eds. B. Ellerbroek & D. Bonaccini Calia, 6272 (2006).
 21. M. Johns, “The Giant Magellan Telescope (GMT),” Proc. SPIE Ground-based and Airborne Telescopes, ed. L. M. Stepp, 6267 (2006).
 22. D. Fabricant, E. Hertz, W. Brown, B. McLeod, R. Angel & M. Lloyd-Hart, “A wide-field IR spectrograph for the Giant Magellan Telescope,” Proc. SPIE Ground-based and Airborne Instrumentation for Astronomy, eds. I. McLean & M. Iye, 6269 (2006).
 23. F. Wildi, G. Brusa, M. Lloyd-Hart & A. Riccardi, “First light of the 6.5-m MMT adaptive optics system,” Proc. SPIE Astronomical Adaptive Optics Systems and Applications, eds. R. Tyson & M. Lloyd-Hart, 5169, 17-25 (2003).
 24. G. Brusa, A. Riccardi, F. Wildi, M. Lloyd-Hart, H. Martin, R. Allen, D. Fisher, D. Miller, R. Biasi, D. Gallieni, & F. Zocchi, “MMT adaptive secondary: first AO closed-loop results,” Proc. SPIE Astronomical Adaptive Optics Systems and Applications, eds. R. Tyson & M. Lloyd-Hart, 5169, 26-36 (2003).
 25. T. Stalcup, R. Angel, M. Lloyd-Hart & M. Rademacher, “Status of the MMT Observatory multiple laser beacon projector,” these proceedings.
 26. J. Georges, P. Mallik, T. Stalcup, R. Angel & R. Sarlot, “Design and testing of a dynamic refocus system for Rayleigh laser beacons,” Proc. SPIE Adaptive Optical System Technologies II, eds. P. Wizinowich & D. Bonaccini Calia, 4839, 473-483 (2002).
 27. C. Baranec, “Astronomical adaptive optics using multiple laser guide stars,” PhD dissertation, University of Arizona (2007).
 28. M. Lloyd-Hart, T. Stalcup, C. Baranec, N. M. Milton, M. Rademacher, M. Snyder, M. Meyer & D. Eisenstein, “Scientific goals for the MMT’s multi-laser-guided adaptive optics,” Proc. SPIE Advances in Adaptive Optics II, eds. B. Ellerbroek & D. Bonaccini Calia, 6272 (2006).
 29. D. McCarthy, J. Ge, J. Hinz, R. Finn & S. de Jong, “PISCES: A Wide-Field, 1-2.5 μm Camera for Large-Aperture Telescopes,” Publ. Astron. Soc. Pac. 113, 353-361 (2001).
 30. M. Freed, P. Hinz, M. Meyer, N. M. Milton & M. Lloyd-Hart, “Clio: A 5 micron camera for the detection of giant exoplanets,” Proc. SPIE Ground-based Instrumentation for Astronomy, eds. A. Moorwood & M. Iye, 5492, 1561-1571 (2004).
 31. S. Sivanandam, P. Hinz, A. Heinze, M. Freed & A. Breuninger, “Clio: a 3-5 micron AO planet-finding camera,” Proc. SPIE Ground-based and Airborne Instrumentation for Astronomy, eds. I. McLean & M. Iye, 6269 (2006).
 32. D. McCarthy, J. Burge, R. Angel, J. Ge, R. Sarlot, B. Fitz-Patrick & J. Hinz, “ARIES: Arizona infrared imager and echelle spectrograph,” Proc. SPIE Infrared Astronomical Instrumentation, ed. A. Fowler, 3354, 750-754 (1998).
 33. P. Hinz, R. Angel, N. Woolf, W. Hoffmann & D. McCarthy, “BLINC: a testbed for nulling interferometry in the thermal infrared,” Proc. SPIE Interferometry in Optical Astronomy, eds. P. Lena & A. Quirrenbach, 4006, 349-353 (2000).
 34. C. Baranec, M. Lloyd-Hart & N. M. Milton, “Ground-layer wave front reconstruction from multiple natural guide stars,” Astrophys. J. 661, 1332-1338 (2007).

35. C. Baranec, M. Lloyd-Hart, N. M. Milton, T. Stalcup, M. Snyder & R. Angel, "Tomographic reconstruction of stellar wavefronts from multiple laser guide stars," Proc. SPIE Advances in Adaptive Optics II, eds. B. Ellerbroek & D. Bonaccini Calia, 6272 (2006).
36. P. McGuire, M. Lloyd-Hart, R. Angel, G. Angeli, R. Johnson, B. Fitzpatrick, W. Davison, R. Sarlot, C. Bresloff, J. Hughes, S. Miller, P. Schaller, F. Wildi, M. Kenworthy, R. Cordova, M. Rademacher, M. Rascon, J. Burge, B. Stamper, C. Zhao, P. Salinari, C. Del Vecchio, A. Riccardi, G. Brusa-Zappellini, R. Biasi, M. Andrighttoni, D. Gallieni, C. Franchini, D. Sandler & T. Barrett, "Full-system laboratory testing of the F/15 deformable secondary mirror for the new MMT adaptive optics system," Proc. SPIE Adaptive Optics Systems and Technology, eds. R. Fugate & R. Tyson, 3762, 28-37, (1999).
37. R. Biasi, L. Fini, P. Mantegazza, V. Bilotti, F. Gori & D. Gallieni, "Control electronics for an adaptive secondary mirror," Proc. SPIE Adaptive Optical System Technologies, eds. D. Bonaccini & R. Tyson, 3353, 1193-1201 (1998).
38. G. Brusa, A. Riccardi, S. Ragland, S. Esposito, C. Del Vecchio, L. Fini, P. Stefanni, V. Biliotti, P. Ranfagni, P. Salinari, D. Gallieni, R. Biasi, P. Mantegazza, G. Sciocco, G. Noviello & S. Invernizzi, "Adaptive secondary P30 prototype: laboratory results," Proc. SPIE Adaptive Optical System Technologies, eds. D. Bonaccini & R. Tyson, 3353, 764-775 (1998).
39. C. Baranec, M. Lloyd-Hart & M. Meyer, "Loki: a ground-layer adaptive optics high-resolution near-infrared survey camera," these proceedings.